# Experimental limit for the charge of the free neutron

J. Baumann
*Experimentalphysik I, Universität Bayreuth, D-8580 Bayreuth, Federal Republic of Germany*

R. Gähler
*Physik-Department E21 der Technischen Universität München, D-8046 Garching, Federal Republic of Germany*

J. Kalus
*Experimentalphysik I, Universität Bayreuth, D-8580 Bayreuth, Federal Republic of Germany*

W. Mampe
*Institut Laue-Langevin, 156X, F-38042 Grenoble Cedex, France*
(Received 12 November 1987)

In agreement with the commonly accepted neutrality of the free neutron, its charge $q_n$ was found to be $(-0.4\pm1.1)\times10^{-21}$ electron charges. This value lowers the present upper limit by more than one order of magnitude. In the experiment a beam of cold neutrons with wavelengths between 1.2 and about 3 nm was passed through a strong electric field over a length of 9 m and a beam deflection with respect to the applied field direction was searched for. In order to increase the sensitivity of the apparatus, an achromatic neutron optical imaging system consisting of curved mirrors and multislits was used.

## I. INTRODUCTION

Electric charges determine the strength of the electromagnetic interaction of particles. By virtue of the law of conservation of charge, it acts as a quantum number controlling the possibility that a particular reaction can take place or not. In this respect electric charge is fundamentally different from baryon and lepton numbers, which are merely quantum numbers characterizing the state of particles and do not play the role of interaction constants.[1]

The commonly accepted symmetry of the electric charge is based on experience. A violation of this symmetry, implying a neutron charge $q_n\neq0$, would have several important consequences. The conservation of baryons would follow from the conservation of electric charge rather than being an independent principle.[2] Assuming a finite neutron charge, a speculative neutron-antineutron transition, as predicted in some unified theories, is forbidden if charge conservation is valid.[3]

If charge conservation is violated, experiments searching for $n\bar{n}$ transitions would be influenced by the mere existence of an electrostatic potential $V$. This gives rise to a change in energy of $E_c=2q_nV$ when a neutron with charge $q_n$ transforms into its antiparticle (charge $-q_n$). If $E_c$ exceeds $10^{-14}$ eV (Ref. 4), the $n\bar{n}$ transition probability could be severely suppressed. The absolute value of the electrostatic potential $V$ is not known, but it plays a role in charge-nonconserving reactions [the potential difference across the atmosphere is already $4\times10^5$ V (Ref. 5)]. In case of charge conservation, the invariance of physics under gauge transformation holds and only differences in $V$ are accessible. Charge-nonconserving effects which clearly violate Maxwell's equations (see, for example, Ref. 6) are postulated by several authors on the basis of grand unified theories.[7–12] One further speculation might be that charge is conserved in $n\bar{n}$ transitions, but only $CP$ is violated, and for this case the potential plays no role.

There have been many measurements in the past testing the neutrality of atoms and bulk material, and in this way only the sum of proton, electron, and neutron charge is determined. From these indirect measurements, a residual neutron charge of less than $10^{-21}q_e$ has been deduced. Direct measurements of the neutron charge have also been made and all of these rely on a possible deflection of slow neutrons in a strong electric field. A review of the various experiments has been given by Petley.[13] Until now the indirect measurements have led to values for the upper limit of the neutron charge which are much lower than the direct measurements. With our present result of $q_n=(-0.4\pm1.1)\times10^{-21}q_e$ obtained in a beam-deflection experiment with free neutrons, we have reached a sensitivity equivalent to that of the indirect methods. According to Shull, Billmann, and Wedgwood, we should face the possibility "of a free charge being slightly different in magnitude at this small level of charge difference when particles are amalgamated in an atom."[14]

## II. MEASURING PRINCIPLE

As in earlier measurements, we have looked for a possible deflection of slow neutrons passing through a strong electric field perpendicular to the beam direction. For a hypothetical neutron charge $q_n$, we expect a defection $y$,

$$y=\frac{q_nE_0L^2}{2mv^2}\ , \tag{1}$$

 

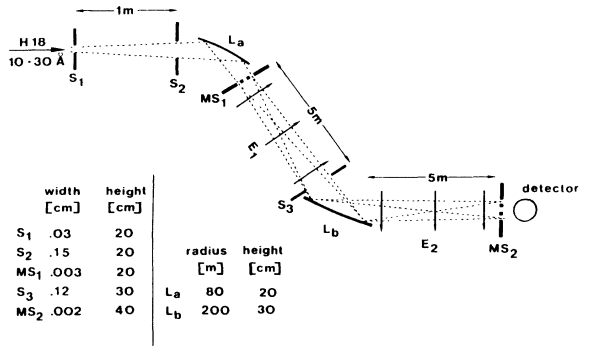


FIG. 1. The design of the deflection apparatus. $MS_1$ and $MS_2$ is a multislit system with 31 slits, 30 $\mu$m wide, separated by 30-$\mu$m-wide absorbing zones. For clarity the dimensions and angles of deflection are not to scale.

with $E_0$ being the electric field applied over the length $L$ and $v$ the neutron velocity.

In the following considerations we assume a Gaussian beam profile with a full width at half maximum of $2\omega_0$. With a detector slit positioned on the steep slope of this intensity profile, a beam deflection $y$ is measured from the difference $\Delta N$ in counting rate for opposite directions of the applied electric field. Assuming a deflection $y$ much smaller than the width of the profile, $\Delta N$ is proportional to this deflection. As shown in Refs. 15 and 16, the uncertainty in $y$ is given by

$$\sigma_y = \frac{\omega_0}{\sqrt{N^* t}} , \tag{2}$$

where $N^* t$ denotes the total neutron counts. $N^*$ and $t$ are the counting rate and the measuring time, respectively.

An improved neutron optical imaging system, as described previously,[17] was used to form a narrow beam with high intensity (Fig. 1). A focusing system consisting of achromatic cylindrical mirrors of high precision permits imaging of an object, the multislit $MS_1$ consisting of 31 slits, with unit magnification into the plane of a second multislit $MS_2$. This image is shown in Fig. 2 as taken by scanning with a single 10-$\mu$m slit. The existence of a

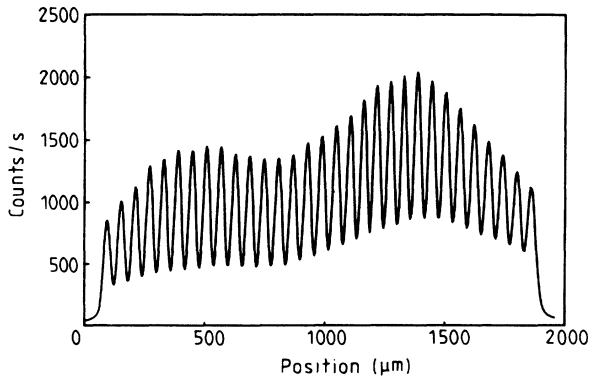


FIG. 2. The image of the multislit system at position $MS_2$ as scanned with a single 10-$\mu$m slit $S_4$.

finite neutron charge would cause a lateral deflection of this image. With the multislit $MS_2$ straddling all of the slope positions on one side of the image, a possible deflection of these 31 lines is sensed simultaneously. Curved, totally reflecting mirrors were used to provide the focusing and, since these are achromatic, a broad neutron spectrum could be used.

## III. DESCRIPTION OF THE INSTRUMENT

### A. The neutron optical imaging system

In the front part of the imaging system (Fig. 1) a condenser (slits $S_1, S_2$, and mirror $L_a$) forms a slightly converging neutron beam by imaging slit $S_1$ with fivefold magnification into the plane of the second mirror $L_b$. The mirror $L_b$ images the object (multislit $MS_1$) with unit magnification into the plane of a second multislit $MS_2$, 10 m from $MS_1$. Between both multislits the neutrons pass through the electric deflection field system having a 3-mm spacing between its electrodes. The condenser in front of $MS_1$ confines the beam profile to a width of about 2 mm and prevents neutrons from striking the electrodes.

As lenses we chose cylindrically shaped mirrors to avoid chromatic aberration. The maximum grazing angle for total reflection is given by $\delta_0 = \lambda(nb/\pi)^{1/2}$, where $n$ is the nuclear density and $b$ the coherent scattering length of the surface material. The mirror surfaces were prepared with $^{58}$Ni because of its unusually large coherent scattering length, and for this we obtain $\delta_0 = 1.23°$ for $\lambda = 1.2$ nm. For the mirror $L_a$ this angle $\delta_0$ was used as the angle of incidence. The mirror surfaces were deposited on a base of Zerodur, chosen because of its very low thermal-expansion coefficient.

The image reversing property of the cylindrical mirror $L_b$ corrects for the deviation $y_c$ caused by the Coriolis force over the 10-m-long flight path from $MS_1$ to $MS_2$, which by calculation would be 25.6 $\mu$m for $\lambda = 2.0$ nm. The multislits consist of 30-$\mu$m-wide openings separated by 30-$\mu$m-wide absorbing zones. The absorbing zones were prepared by evaporation of a 630-nm layer of $^{157}$Gd on a 1.5-mm-thick quartz plate and show a nominal absorption of 97.5% for neutrons of 1.5-nm wavelength.

The optimum sensitivity for detecting a deflection of the image in the plane of multislit $MS_2$ was achieved with the following arrangement. The second multislit $MS_2$ consists of two parallel multislit plates similar to $MS_1$ separated by 6.5 mm. By slight rotation of this assembly around a vertical axis, the ratio of the slit width to the width of the absorbing zones can be changed continuously between zero and 1 without changing the lattice constant to first order. As the optimum slit width for detecting a deflection, we determined a value of 14 $\mu$m. The counting rate measured behind $MS_2$ was 30 000 $n$/sec. A shift of the image of 1 $\mu$m causes a change in counting rate of about 900 $n$/sec (Fig. 3). As shown in Fig. 1, the height of the optical components increases from 0.2 m ($S_1$) to 0.4 m ($MS_2$) to allow for the vertical divergence of the neutron beam. A more detailed description of the optical layout has been given in a previous paper.[18] A $BF_3$

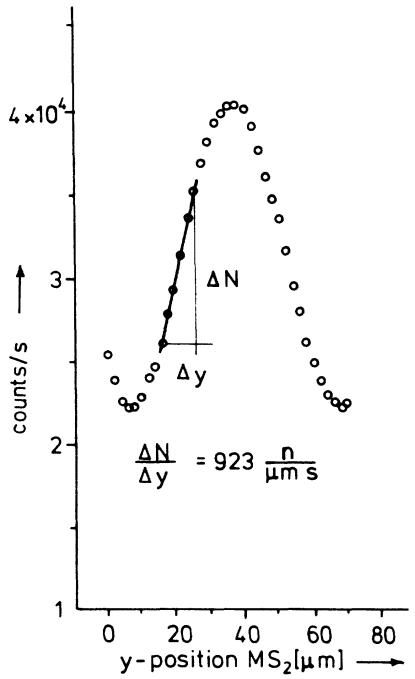


FIG. 3. The image of the multislit system scanned with the multislit $MS_2$ with 14-$\mu$m width of each single slit.

counter with low $^{10}B$ content was used as the neutron detector with a surrounding shielding of a 30-cm-thick paraffin-boron mixture having an entrance window of 4-mm width.

The supports for all optical elements from $L_a$ to $MS_2$ are granite blocks, which are mounted on a vibration isolated and heat treated optical bench of 10-m length and about 4000-kg weight. The bench, a rectangular steel tube, was filled with water to increase its heat capacity and was surrounded by 5-cm polystyrene and a thermal isolation foil. Movement of this bench caused by currents of air from the reactor air conditioning were successfully reduced by plastic foils surrounding the apparatus. It was established that drifts in the alignment of the optical elements did not exceed a few microns per day.

Because of aberrations in the optical system, the image of each single slit will have Gaussian shape to first approximation. The broadening within the image structure arises from the precision of the mirror itself, from the lateral dimensions of the object, and from movements of the optical components especially those from vibration of the mirror $L_b$ about a vertical axis.

For $L_b$ the radius of curvature is given by $R_b = 200 \pm 0.5$ m and this implies that deviations from the ideal cylindrical shape are restricted to about $\pm 10$ nm over the entire mirror surface of 300 by 80 mm. At present this is about the ultimate precision attainable in fabricating such a mirror. Together with spherical aberration we expect an image error of about 15 $\mu$m for an ideal adjustment of all optical components. Thus a width of 30 $\mu$m for one slit and a distance of 60 $\mu$m between the slits seemed to be reasonable in the design of the object multislit.

The lateral dimensions of the whole object (in our case the number of slits to be used) are limited by optical distortion. The focal length of a cylindrical mirror is given by

$$f = (R \sin\theta)/2 \quad \text{or} \quad \Delta f/f = \Delta\theta/\theta \quad \text{for small } \theta\ , \tag{3}$$

where $\Delta\theta$ denotes the variation of the angle of incidence due to the lateral dimensions of the object which is about the size of the multislit consisting of 31 slits. For a tolerable image smearing of 10 $\mu$m, a lens aperture of $4 \times 10^{-4}$ and a mean angle of incidence of $\theta_0 = 1.2°$, we can tolerate an object width of 2 mm.

### B. Deflection of a charge $q_n$ in an electric field

Equation (1) is valid for a beam which travels freely over the length $L$ in an electric field. For our optical device some modifications are required. First, the electric field is divided by the mirror $L_b$ into two sections of equal length $L_1/2$. The optical components themselves are excluded from the field. For a symmetric arrangement of these two fields with respect to the optical elements, the term $L^2$ in Eq. (1) is replaced by $L_0 L_1$ with $L_0$ being the flight path between $MS_1$ and $MS_2$. Second, the deflection $y$ is smaller than without imaging. Because of the focusing properties of the mirror $L_b$, the flight path is bent back to the optical axis. In our setup with unit magnification, this implies that the deflection is reduced by a factor of 2.

For a hypothetical neutron charge $q_n = 10^{-21} q_e$, we expect a deflection of

$$y = 2.3\ (14.7) \times 10^{-10}\ \text{m} \tag{4}$$

for neutrons with wavelengths of 1.2 (3) nm respectively, $E_0 = \pm 6 \times 10^6$ V/m, $L_0 = 10$ m, and $L_1 = 9$ m.

### C. The neutron spectrum

Compared to the previously used optical system with its severely chromatic lens,[15,16] our present arrangement allows for a broad spectral width. We use the full spectrum from the cold-neutron guide H18 of the high-flux reactor in Grenoble down to a wavelength of $\lambda_0 = 1.2$ nm, determined by the cutoff wavelength of the mirror surface material at the chosen angle of incidence $\delta_0$ (Fig. 4). ($\theta_0 = 1.23°$ for $\lambda_0$ with $^{58}Ni$ as surface reflecting material.)

The deflection of a charge $q_n$ in a static $E$ field is proportional to $1/v^2$ and hence proportional to $\lambda^2$. The sensitivity for the measurement remains unchanged if all neutrons are characterized by one wavelength $\lambda_m$ instead of the given distribution $\Theta(\lambda)$:

$$\lambda_m^2 = \langle \lambda^2 \rangle_{\text{av}} = \frac{\int \lambda^2 \Theta(\lambda) d\lambda}{\int \Theta(\lambda) d\lambda}\ , \tag{5}$$

which indicates that the weighting of the different wavelengths is proportional to their deflection.

From a time-of-flight measurement (shown in Fig. 4) we get for $\lambda_m$ a value of 1.74 nm. Note that for the present experimental arrangement the sensitivity for a

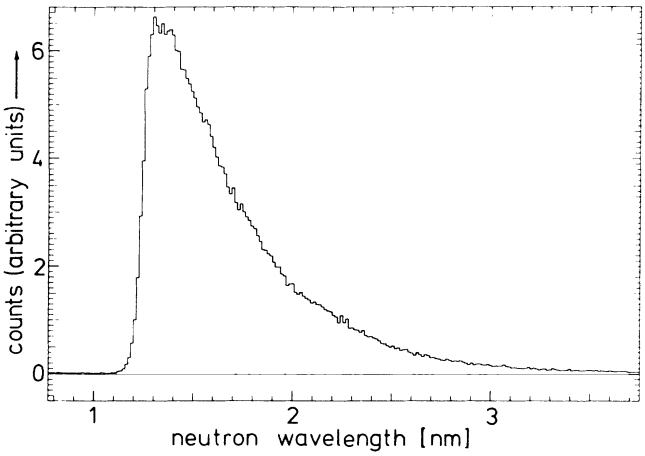


FIG. 4. The spectrum of the neutrons measured with a time-of-flight method.

charge measurement should be independent of the cutoff wavelength $\lambda_0$ of the mirror, provided that the neutron spectrum (from $\lambda_0$ to $\infty$) is proportional to $1/\lambda^5$. This is valid for $\lambda \ll \lambda_{th}$ with $\lambda_{th}$ being the mean wavelength of the Maxwellian distribution. In this case the intensity $N(\lambda_0)$ and the mean wavelength $\lambda_m$ depend only upon the cutoff wavelength $\lambda_0$:

$$N(\lambda_0) \sim \int_{\lambda_0}^{\infty} \Theta(\lambda) d\lambda = \int_{\lambda_0}^{\infty} c(1/\lambda^5) d\lambda = c/4\lambda_0^4 , \quad (6)$$

where $c$ is proportional to the reactor power and inversely proportional to the square of the moderator temperature. Using the $1/\lambda^5$ law for the neutron spectrum we get, from Eq. (5),

$$\lambda_m^2 = 2\lambda_0^2 . \quad (7)$$

By setting the deflection [Eq. (1)] equal to the measurable shift $\sigma_y$ [Eq. (2)] we deduce, for a measurable neutron charge $q_n$,

$$q_n(\text{minimal}) \sim \frac{1}{\lambda_m^2 [N(\lambda_0)]^{1/2}} = \frac{(4\lambda_0^4)^{1/2}}{2\lambda_0^2 c^{1/2}} = \frac{1}{c^{1/2}} , \quad (8)$$

which is independent of $\lambda_0$.

### D. The electric field

The present experiment was performed with the same electrostatic deflection system used in our previous experiment.[15,16] The electrodes consist of two 4.5-m-long stainless steel tubes with rectangular cross section. Their surfaces were milled to a precision of about 0.2 mm over the whole area. The electrodes are mounted inside vacuum chambers of 0.8 m diameter and 4.6 m length. An improved mechanical support for the vacuum chambers allows a precise adjustment of the electrodes relative to the neutron beam. A more detailed description is given in Refs. 15 and 16.

Several tests with different electrode materials and specially treated surfaces showed no significant increase of the maximum electric field strength, which was limited partly by problems with cleaning the large electrode areas.

During the charge measurement the vacuum in the two chambers was maintained lower then $1.3 \times 10^{-3}$ Pa. With an electrode gap of 3 mm and an applied electric field of $\pm 6$ kV/mm, the number of high-voltage breakdown events was less than 10 per hour.

## IV. MEASUREMENTS AND RESULTS

### A. Measurement procedure

The neutron-charge measurement reported here belongs to a certain class of experiments where a tiny effect is searched for by repeated reversal of one physical parameter. In our case we look for a difference in intensity for opposite directions of the electric field. The charge measurement was performed with a large number of reversal cycles and within each cycle the counting rate behind the detector slits was measured for 10 sec in one field direction and 10 sec in the other field direction. Including the time to charge and discharge the electrodes, one cycle lasted about one-half minute. The short measuring time for each field direction was chosen in order to reduce systematical errors caused by long-time drifts of the position of the image. Several hundred to several thousand of such cycles were combined to form a run. In cases where a breakdown of the high voltage occurred, the actual measurement was stopped and the counting rate was deleted. The quality of the image was checked regularly in order to verify the deflection sensitivity of the apparatus.

### B. Data, analysis, and results

During two reactor periods of 44 days each, 91 runs were carried out with 26 being performed with only one of the electrode pairs in operation (see Sec. V). For each run the difference in counting rate for the two field directions ($\Delta N = N_- - N_+$) was calculated and compared in a first analysis to the statistical error given by $(N_- + N_+)^{1/2}$. This procedure provides a test for the presence of eventual systematic errors.

A detailed analysis of the data showed that the distribution of the $\Delta N$ values for each measuring cycle was broader than we would expect assuming only statistical errors $\sigma_{stat}$. A $\chi^2$ test for the actual $\Delta N$ values of each cycle and for $\Delta N = 0$ as the expectation value results in a mean value of 1.39 for $\chi^2$. This indicates the presence of an additional systematic error $\sigma_{sys} = 0.6\sigma_{stat}$. The distribution of the actual $\chi^2$ for the different runs around the mean value of 1.39 is in accordance with the expectation for a normal distribution. A similar $\chi^2$ test was performed for the monitor counting rate. This suggested that the change of the neutron flux was one of the main reasons for this systematic error. The monitor count rate is proportional to the intensity of the neutrons entering the deflection apparatus and was measured in front of slit $S_1$ by means of a transmission counter. Variations of this

monitor count rate arise from the control of the reactor power. These variations account for about 50% of $\sigma_{sys}$. By taking into account the systematic error of $\sigma_{sys}=0.6\sigma_{stat}$ the final result is

$$q_n=q_e(-0.6\pm1.1)\times10^{-21} \quad (68\% \text{ confidence}) . \quad (9)$$

It turned out that the quality of the runs depended upon factors additional to the measuring time $t$ (i.e., the number of cycles in the run). Therefore we made an independent analysis of the data taking into account the actual fluctuation of the data. These results are collected in Fig. 5. As the final result of this analysis we obtained

$$q_n=q_e(-0.4\pm1.1)\times10^{-21} \quad (68\% \text{ confidence}) . \quad (10)$$

The difference in the values of Eqs. (9) and (10) stems from the fact that the weighting of the individual runs is different for the two data evaluations.

The errors from the determination of the mean wavelength $\lambda_m$, the lengths $L_0, L_1$, and the electric field $E_0$ are negligible compared to the statistical errors.

A strange effect, which is not fully understood, should be mentioned. The image quality showed a periodic variation of frequency between $2\times10^{-3}$ and $8\times10^{-4}$ Hz over periods of many days. The amplitude of these "oscillations" was about 1% of the counting rate and was in antiphase at the maxima and at the minima of the profiles. The counting rate of the total image remained constant. Many tests were carried out to look for the origin of these "oscillations." Finally we obtained some indication that small movements of the mirror $L_b$ might have caused this effect. Changing the support of the mirror with some extra weight ($\simeq$10-kg lead) we were able to change reproducibly the amplitudes of these oscillations, but their origin was not found.

The charge measurement was not influenced by this effect, because these oscillations were not present in the slope of the image, where the multislit $MS_2$ was positioned for sensing a systematic deflection due to the $E$ field.

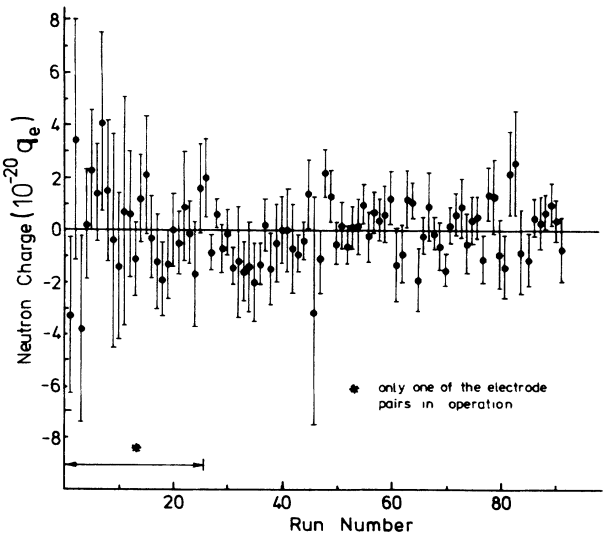


FIG. 5. Diagram of all individual measurements (runs) of the neutron charge. The error bars indicated are calculated from the distribution of the $\Delta N$ values of each measuring cycle. The run numbers are ordered chronologically.

## V. SYSTEMATIC ERRORS DUE TO THE ELECTRIC FIELD

In our opinion the most sensitive parameter of the optic system is the angle of mirror $L_b$ with respect to the beam axis. A systematic change of this angle by $10^{-10}$ rad coupled to the direction of the electrostatic fields should simulate a beam deflection and thus a neutron charge of the order of magnitude we were looking for. The mirror with its solid support is positioned symmetrically between the two electric field regions which are screened by the vacuum chambers. Nevertheless, disturbance of the mirror position caused by these fields, due to leakage currents or due to the supply cables might not be completely excluded on this scale of angular sensitivity. To check this, about 30% of the runs were performed with maximum field in front of the mirror but no field behind, which should somehow vary the effect, if caused by this interaction. The analysis of these data gave $q_n=q_e(-0.2\pm3.3)\times10^{-21}$ (68% confidence) which indicates no systematic coupling of the $E$ field to the mirror position.

Apart from a neutron charge, the magnetic moment and the intrinsic structure of the neutron can also give rise to a deflection in the electric field.[19] Most of these forces are coupled to the field direction and hence are experimentally unseparable from a force on a possible neutron charge. A calculation of these undesired effects has been given in Ref. 15. It is shown that the deflection caused by a neutron charge $q_n=10^{-21}q_e$ (the sensitivity of the present experiment) is large compared to other deflections. Assuming a total polarized beam, only the "$\mathbf{E}\times\mathbf{v}$" term (Ref. 20) ($v$ is the velocity of the neutrons) causes a force on the magnetic dipole moment of the neutron which is of the same order of magnitude as the force acting on a neutron charge of $10^{-21}q_e$ in an electric field of $6\times10^6$ V/m. Because of the relativistic field equations, a neutron moving with velocity $\mathbf{v}$ in an $\mathbf{E}$ field sees a magnetic field $\mathbf{B}=(1/c^2)\mathbf{E}\times\mathbf{v}$. With a neutron beam traveling in the $x$ direction through a transverse homogeneous electric field $\mathbf{E}=\mathbf{E}_y$ the neutron sees only a magnetic field in the $z$ direction which cannot give rise to a lateral deflection of the beam.

For a closer examination of this effect, inhomogeneous $\mathbf{E}$ fields and the beam divergence must be taken into account. In this case, the $\mathbf{B}$ field arising in the $y$ direction can be written as

$$B_y=\mathbf{e}_y(E_zv_x-E_xv_z)(1/c^2) . \quad (11)$$

As $v_x$ is about 2 orders of magnitude larger than $v_z$ only the term $E_zv_x$ has to be considered. Electric fields in the $z$ direction can occur by a small tilting of the electrode plates with respect to each other. Assuming that the electrode gap at the upper edge of the plates is about 1 mm smaller than at the lower one, the resulting electric field in the $z$ direction is given by

$$E_z = E_0 \sin\alpha \ , \tag{12}$$

where $\alpha$ is the tilting angle between the two electrode plates ($\simeq 3\times 10^{-3}$ rad). Hence the resulting magnetic field can be written in the form

$$B_y = E_0 \alpha v_x / c^2 \ . \tag{13}$$

With a field gradient $\delta B_y/\delta y \simeq B_y/d$ ($d$ is the mean distance between the electrode plates), the force acting on the magnetic dipole moment of the neutron $\mu_n$ is given by

$$\mu_n (E_0 \alpha v_x / dc^2) \simeq 1.3\times 10^{-34} \text{ N} \ . \tag{14}$$

This is smaller than the force acting on a neutron charge of $10^{-21} q_e$:

$$q_n E_0 = 10^{-21}\times 1.6\times 10^{-19}\times 6\times 10^6 \simeq 1\times 10^{-33} \text{ N} \ . \tag{15}$$

A realistic estimation for the polarization of the neutron beam used in the experiment reduces this effect by at least another order of magnitude.

## VI. CONCLUSIONS

The reported value for the charge of the free neutron is lower than the recently known upper limit by more than one order of magnitude. As shown in Secs. IV B and V, further improvement of this value with a more refined apparatus would require a major effort.

## ACKNOWLEDGMENTS

We are highly indebted to the workshop of the University of Bayreuth for fabrication of most of the apparatus, to P. Hurych and W. Griessl for electronic assistance, and to the director and the staff of the Institute Laue Langevin for help and encouragement. This work has been supported by the Bundesministerium für Forschung und Technologie Grant No. 06 BT 551.

[1] A. I. Akhiezer and M. P. Rekalo, Usp. Fiz. Nauk. **114**, 487 (1975) [Sov. Phys. Usp. **17**, 864 (1975)].
[2] G. Feinberg and M. Goldhaber, Proc. Natl. Acad. Sci. U.S.A. **45**, 1301 (1959).
[3] S. L. Glashow, in *Proceedings of Neutrino 79,* edited by A. Haatuft and C. Jarlskog (Bergen, Norway, 1979), Vol. I, p. 518.
[4] G. Costa and F. Zwirner, Riv. Nuovo Cimento **9**, 43 (1986).
[5] R. P. Feynman, *Lectures on Physics* (Addison-Wesley, Reading, MA, 1973), Vol. II.
[6] E. Comay, Phys. Rev. D **33**, 2492 (1986).
[7] W. J. Marciano and I. J. Muzinich, Phys. Rev. Lett. **50**, 1035 (1983).
[8] T. M. Yan, Phys. Rev. D **28**, 1496 (1983).
[9] R. Jengo, Phys. Lett. **145B**, 353 (1984).
[10] G. Galucci and G. Vedovato, Z. Phys. C **27**, 377 (1983).
[11] R. Jengo, Nucl. Phys. **B252**, 217 (1985).
[12] G. Galucci and G. Vedovato, Z. Phys. C **29**, 111 (1985).
[13] B. W. Petley, *The Fundamental Physical Constants and the Frontier of Measurement* (Hilger, London, 1985).
[14] C. G. Shull, K. W. Billmann, and F. A. Wedgwood, Phys. Rev. **153**, 1415 (1967).
[15] R. Gähler, J. Kalus, W. Mampe, Phys. Rev. D **25**, 2887 (1982).
[16] R. Gähler, J. Kalus, and W. Mampe, in *Precision Measurements and Fundamental Constants II,* edited by B. N. Taylor and W. D. Phillips (Natl. Bur. Standards, Spec. Publ. **677**, 1984).
[17] J. Kalus and R. Gähler, J. Phys. (Paris) Colloq. **45**, C3-17 (1984).
[18] J. Baumann, R. Gähler, J. Kalus, and W. Mampe, J. Phys. E **20**, 448 (1987).
[19] H. Rauch, in *Neutron Interferometry,* edited by K. Bonse and H. Rauch (Oxford University Press, Oxford, 1979), p. 161.
[20] J. Schwinger, Phys. Rev. **69**, 681 (1948).